

Computational Study of Air-Cooled Servers with Improved Ducting and Chassis  
Re-design

by

HIMANSHU MODI

Presented to the Faculty of the Graduate School of  
The University of Texas at Arlington in Partial Fulfillment  
of the Requirements  
for the Degree of

MASTER OF SCIENCE IN MECHANICAL ENGINEERING

THE UNIVERSITY OF TEXAS AT ARLINGTON

MAY 2020

Copyright © by HIMANSHU MODI 2020  
All Rights Reserved

## ACKNOWLEDGEMENTS

I would like to thank Dr. Dereje Agonafer who helped throughout my work. His continuous guidance and support throughout my thesis and research at The University of Texas at Arlington helped me to cross every hurdle. I would also like to thank Dr. Abdolhossein Haji-Sheikh and Dr. Miguel A. Amaya for evaluating my work as committee members.

I am obliged and thankful to Uschas Chowdhury for sharing his technical expertise throughout my research work. His mentoring and support has played an important role in finishing this work

My special thanks to my parents Mr. Girischandra Modi and Ms. Ketaki Modi, my brother Ravi, my sister Dr. Tulsi and Namarata Modi for serving my motivation and inspiration. I endlessly thank them for providing an opportunity to pursue my goals in life.

I would also like to thank Almighty God for providing me the strength, inspiration and courage to face any situations in life to reach my goals.

May 15, 2020

## ABSTRACT

### Computational Study of Air-Cooled Servers with Improved Ducting and Chassis Re-design

HIMANSHU MODI, M.S.

The University of Texas at Arlington, 2020

Supervising Professor: Dr.Dereje Agonafer

In recent years there has been a phenomenal increase in cloud computing, networking, virtualization, and storage which has led to an increase in demand for data centers. To meet this demand, there is a need for the latest computing nodes which causes an increase in power consumption. The cooling system occupy almost 40% portion of total energy consumption. Per ASHRAE TC 9.9, IT equipment needs to operate within recommended and allowable temperatures and humidity zone based on the circumstances. As the inlet air temperature increases, fan power consumption increases too and the Central Processing Units (CPUs) and high heat-generating components inside each server need to operate at their respective reliable temperatures. Design modifications for duct and chassis can be made to lower the junction temperatures for maximum utilization of CPU and memory. In this study, parametric optimization was performed for improvements in the duct and chassis of an air-cooled server (Cisco C220 M3) to find a sweet spot between the trade-off of airflow rate and junction temperature. For this study, the server used is the 1U height server with 2 CPUs, 16 Dual In-line Memory (DIMMs), 1 Platform Controller Hub (PCH), and

5 hot-swappable 40 mm fans. Initially, the study discusses the improvements in the duct design to guide cooler air inside the server decreasing maximum surface temperatures of components. Later, the study involves vent opening on the sides of the chassis to add fresh cold air with the inlet air stream with the help of the new duct to further reduce the junction temperature. Parametrization was performed for the hole diameters, area of perforation, and operating RPM for fans while considering EMI best practices and following guidelines to avoid stress concentration on mounting rail and chassis. Overall, the study evaluates the new duct design and the redesigned chassis by showcasing the simulated results including the fan power consumption, temperatures of the components at different inlet air temperatures.

## TABLE OF CONTENTS

ACKNOWLEDGEMENTS . . . . .	iv
ABSTRACT . . . . .	v
LIST OF ILLUSTRATIONS . . . . .	ix
LIST OF TABLES . . . . .	xi
Chapter	Page
<b>1. INTRODUCTION . . . . .</b>	<b>1</b>
<b>1.1 Data center : An Introduction . . . . .</b>	<b>1</b>
<b>1.2 Air Cooling Configuration . . . . .</b>	<b>2</b>
<b>1.3 Thermal Management of Data centers . . . . .</b>	<b>3</b>
<b>1.4 Motivation . . . . .</b>	<b>4</b>
<b>2. Server Under Study . . . . .</b>	<b>6</b>
<b>2.1 Server Description . . . . .</b>	<b>6</b>
<b>2.1.1 Ducting System . . . . .</b>	<b>8</b>
<b>3. Computational Fluid Dynamics (CFD) Analysis . . . . .</b>	<b>10</b>
<b>3.1 Detailed Model of the Baseline Model . . . . .</b>	<b>10</b>
<b>3.1.1 Heatsinks . . . . .</b>	<b>12</b>
<b>3.2 Mesh Sensitivity Analysis . . . . .</b>	<b>13</b>
<b>3.3 Flow Analysis using CFD . . . . .</b>	<b>14</b>
<b>3.3.1 System Resistance curve . . . . .</b>	<b>14</b>
<b>4. Design Improvements . . . . .</b>	<b>17</b>
<b>4.1 Improvement in duct design . . . . .</b>	<b>17</b>
<b>4.2 Improvement in Chassis design . . . . .</b>	<b>20</b>

5. Results . . . . .	23
5.1 Mesh Sensitivity Analysis . . . . .	23
5.2 System Resistance Curve . . . . .	24
5.3 Temperature comparison of baseline and improved design . .	27
5.4 Temperature comparison for different fan speeds and FAR .	28
5.5 Savings achieved in Fan speeds . . . . .	33
5.6 Savings achieved in fan power consumption . . . . .	34
6. CONCLUSION AND FUTURE WORK . . . . .	36
6.1 Conclusion and Discussion . . . . .	36
6.2 Future Work . . . . .	36
REFERENCES . . . . .	37
BIOGRAPHICAL STATEMENT . . . . .	40

## LIST OF ILLUSTRATIONS

Figure	Page
1.1 Typical Data Center Layout [1] . . . . .	3
1.2 Summary of ASHRAE 2011 Thermal Guideline Classes [2] . . . . .	4
2.1 Front View of Cisco C220 [3] . . . . .	6
2.2 Schematic Representation of Server [3] . . . . .	7
2.3 Dimensional model of Fan [4] . . . . .	8
2.4 Isometric View of Duct . . . . .	9
2.5 Top View of Duct . . . . .	9
3.1 Isometric View of CFD Model . . . . .	10
3.2 Top View of CFD Model . . . . .	11
3.3 Rear View of CFD Model . . . . .	11
3.4 Side View of CFD Model . . . . .	12
3.5 Heatsink Model for the server . . . . .	13
3.6 Model with 17M Grid Count . . . . .	14
3.7 Position of Inlet & Outlet Sensor . . . . .	15
3.8 System Resistance curve for the baseline [5] . . . . .	16
4.1 Original Duct . . . . .	18
4.2 Improved Duct . . . . .	19
4.3 Closer View of Vanes inside Duct . . . . .	19
4.4 Vane dimensions . . . . .	20
4.5 Side Vent openings . . . . .	21
4.6 Front View of the Vent . . . . .	22



5.1	Grid independence of study of static pressure . . . . .	23
5.2	Grid independence of study of Component Temperature . . . . .	24
5.3	General representation of system resistance curve [6] . . . . .	25
5.4	Comparison of impedance curve of Baseline Vs Improved Duct . . . . .	26
5.5	Comparison of Resistance curve of baseline model with new model . . . . .	27
5.6	Temperature plot of the baseline and improved design model . . . . .	27
5.7	. . . . .	28
5.8	Placement of sensors . . . . .	29
5.9	Temperature at different vent hole diameter at 67% FAR . . . . .	30
5.10	Temperature at different Vent Hole Diameters at 97 % FAR . . . . .	30
5.11	Temperature of U06 component at different inlet temperature . . . . .	31
5.12	Temperature of U01 component at different inlet temperature . . . . .	31
5.13	Temperature of Chipset at different inlet temperature . . . . .	32
5.14	. . . . .	33
5.15	Fan speeds for the baseline and improved design . . . . .	34
5.16	Fan Power Consumption at Different Air Inlet Temperature . . . . .	35

## LIST OF TABLES

Table	Page
2.1 Components location in Schematic Representation . . . . .	7
3.1 Thermal Design Power of the components . . . . .	12
3.2 Heatsink Specifications . . . . .	13
5.1 Position of Sensors . . . . .	29
5.2 Temperature of U06 Component at different inlet temperature . . . . .	31
5.3 Temperature of U01 at different inlet temperature . . . . .	32
5.4 Temperature of Chipset at different inlet temperature . . . . .	32
5.5 Fan speeds for the baseline and improved design . . . . .	34
5.6 Savings in fan power consumption . . . . .	35

## CHAPTER 1

### INTRODUCTION

#### 1.1 Data center : An Introduction

At its simplest, a Data center in any organization is a facility that houses their critical applications and data. Its design is based on network, computing and storage resources that enables the delivery of sharing applications and data. The core components of data center are switches, routers, firewalls, storage systems, servers, and controllers [7]. As per 2018 study on total energy consumption, it is observed that there is a total energy consumption of 205 terawatt of energy consumed by the data centers which is roughly 1% of energy consumption worldwide which is total of 6% increase in energy consumption worldwide since 2010 [8].

As the servers are required to operate at optimum temperatures it is essential that they work continuously without any maintenance or without stopping the entire data center. Thus, cooling of the data center is important. Due to growing environmental concern and increase in the power consumption has increased the demand of better and more efficient way for cooling the data centers. Production of energy is a worldwide concern and producing sufficient energy while continuing to reduce unwanted pollutant emissions is important [9, 10]. Recent trends toward efficiency improvement and global awareness of climate change caused by  $CO_2$  emission into the atmosphere have led to a renewed effort in the development of more efficient and less environmentally harmful power generation systems [11]. With the increasing demand for the production of energy, researchers are making tremendous effort to produce energy more efficiently while maintaining costs low [12]. So it is indispens-

able to build energy efficient data center which can save energy and efficient at the same time.

## 1.2 Air Cooling Configuration

In an Air-cooled server, for cooling the equipment inside the server are the cooling fans and the heat sinks above the CPU's used to remove the heat. Basically, the heat transfer through the CPU chips occur by the conduction, radiation, and convection process. The fans of the server are generally controlled by the sensors used to check the temperatures of the processors and controls the fan speeds accordingly. The hot air exits the server and enters the hot aisle in the data center and is sent to the Computer Room Air Cooling (CRAC) Unit. Here, the air is cooled to the required inlet temperatures and again sent to the cold aisle of the data center through raised flooring of the room [1]. A typical data center is shown in Figure 1.1. Data centers can also be cooled by oil immersion technology. Ramdas et al. mentioned that immersion cooling technique is used for the thermal management of high-power density data centers to avoid overheating of components like printed circuit board (PCB), electronic packages and failure of servers. However, to use this as a viable cooling technique, the effect of dielectric coolant on the reliability of server components needs to be evaluated [13]. So air cooling configuration still remains the primary technique for cooling data centers.



Figure 1.1: Typical Data Center Layout [1]

### 1.3 Thermal Management of Data centers

The equipment's inside the Data centers consumes lot of power and thus dissipate a large amount. This requires the cooling of the equipment's to operate at optimum temperature. Shah et al. studied the reliability considerations for oil immersion-cooled data centers [14]. There are different challenges involved in immersion cooled data centers. So air cooling is used most of the data centers. In order to achieve optimum temperature and cooling of these equipment's, it is crucial to provide sufficient airflow. For optimum cooling and designing purposes of these data centers American Society of Heating, Refrigerating and Air-Conditioning Engineers .(ASHRAE) TC 9.9 [2] have developed standard guidelines to operate, design , maintain and run data centers at efficient energy consumption's. ASRAE TC 9.9 have provided 4 inlet temperature zones as shown in the figure 1.2.

Classes (a)	Equipment Environmental Specifications							
	Product Operations (b)(c)					Product Power Off (c) (d)		
	Dry-Bulb Temperature (°C) (e) (g)	HumidityRange, non-Condensing (h) (i)	Maximum Dew Point (°C)	Maximum Elevation (m)	Maximum Rate of Change(°C/hr) (f)	Dry-Bulb Temperature (°C)	Relative Humidity (%)	Maximum Dew Point (°C)
<b>Recommended</b> (applies to all A classes, evaluate ITE metrics in this paper for conditions outside this range)								
A1 to A4	18 to 27	5.5°C DP to 60% RH and 15°C DP						
<b>Allowable</b>								
A1	15 to 32	20% to 80% RH	17	3050	5/20	5 to 45	8 to 80	27
A2	10 to 35	20% to 80% RH	21	3050	5/20	5 to 45	8 to 80	27
A3	5 to 40	-12°C DP & 8% RH to 85% RH	24	3050	5/20	5 to 45	8 to 85	27
A4	5 to 45	-12°C DP & 8% RH to 90% RH	24	3050	5/20	5 to 45	8 to 90	27
B	5 to 35	8% RH to 80% RH	28	3050	NA	5 to 45	8 to 80	29
C	5 to 40	8% RH to 80% RH	28	3050	NA	5 to 45	8 to 80	29

Figure 1.2: Summary of ASHRAE 2011 Thermal Guideline Classes [2]

#### 1.4 Motivation

The infrastructure houses number of components and servers. Tushar et al. studied the effect of thermal aging and thermal cycling on the thermal interface materials and found that thermal expansion decreased from approximately 2.5% to 1.2% and after 1000 thermal cycles delamination and major cracks were observed in samples [15]. Misrak et al. studied impact of aging on mechanical properties of thermally conductive gap fillers [16]. Mugdha et al. performed reliability assessment of BGA Solder Joints on different Printed Circuit Boards and found that Megtron PCBs perform better than FR-4 which is a major component electronic equipment [17]. Rahangdale et al. performed solder ball reliability assessment of WLCSP — Power cycling versus thermal cycling [18,19]. It is observed in numerous studies that a small percentage increase in cooling performance at server level can have a large-scale improvement on cooling of the whole data center. An energy Logic model by

Emerson Network Power, reported that one Watt of power saved at the server level extrapolated to as much as 2.84 watts at the facility level [20]. In this study we will be focusing on the improvement of the airflow inside the server by improving the duct design and keeping some of the factors into consideration such as the electromagnetic interference effects on the size of the holes on the vents. The main objective of the study is to reduce cooling power consumption and lower the fan speeds to cool the components of the server. This work involves computational study to establish that an improved duct can reduce the fan speeds and provide a better cooling of the components.

## CHAPTER 2

### Server Under Study

#### 2.1 Server Description

The system considered for the study is Cisco® UCS C220 M3 rack server designed for performance and density over a wide range of business workloads from web serving to distributed database. The server has a 1U form factor with height 1.75in, width 16.92in and depth of 28.5in. The server consists of two CPU's of Intel Xeon E5-M2600 v2 and ME5-2600 processor with a thermal design power (TDP) of 135 Watts. It has 16 DIMMs, up to 8 drives and 2 x 1 GbE LAN-on-motherboard (LOM) ports delivering outstanding levels of density and performance in a compact 1U package.

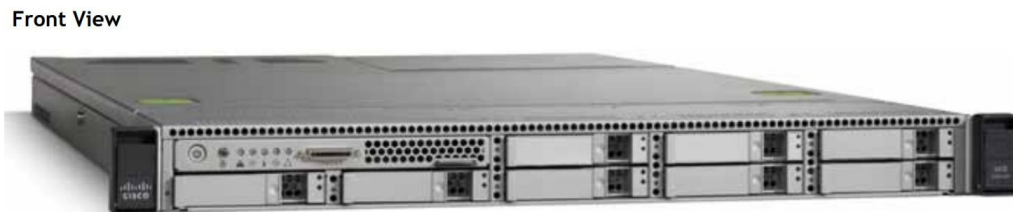


Figure 2.1: Front View of Cisco C220 [3]

The top chassis cover is detachable and can be opened to access the internal components of the server. The figure shows a schematic representation of the components and their location inside the server.



Table 2.1: Components location in Schematic Representation

1	Drives (hot-swappable, accessed through front panel)	10	Trusted platform module socket on motherboard
2	Drive backplane	11	Standard-profile PCIe riser (PCIe slot 1)
3	SuperCap backup unit mounting location	12	Low-profile PCIe riser (PCIe slot 2)
4	Cooling fans (five)	13	Cisco Flexible Flash SD socket SD2 on PCIe riser 2
5	SCU upgrade ROM header (RAID key)	14	Cisco Flexible Flash SD socket SD1 on PCIe riser 2
6	DIMM slots on motherboard (16)	15	Internal USB port
7	CPUs and Heatsinks (two)	16	Power supplies (two, hot-swappable access through rear panel)
8	Integrated RAID on motherboard, and mini-SAS connectors	17	RTC battery on motherboard
9	Mezzanine RAID card, mini-SAS connectors SAS1 and SAS2	18	Software RAID 5 header (RAID key)

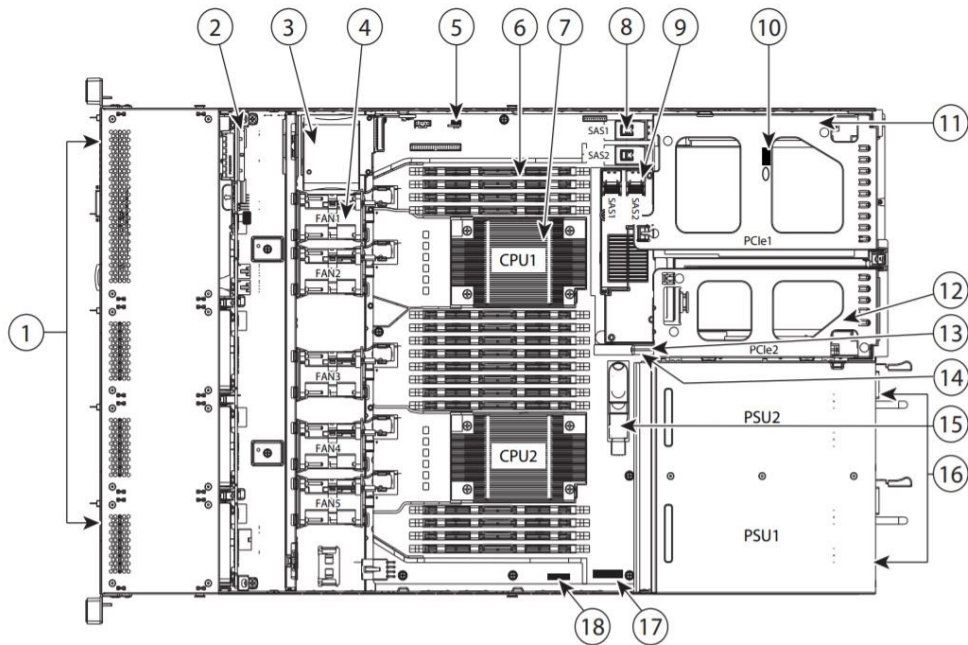


Figure 2.2: Schematic Representation of Server [3]

The server is provided with five fans located at the front end of the server in push configuration which sucks air from the inlet and throws air towards the components. The dimensions of the fans are 40cmX40cmX56cm. The speed of the fans is controlled by the CPU die temperatures with the help of inbuilt fan control algorithms. The schematic diagram of the fan is shown in figure 2.3

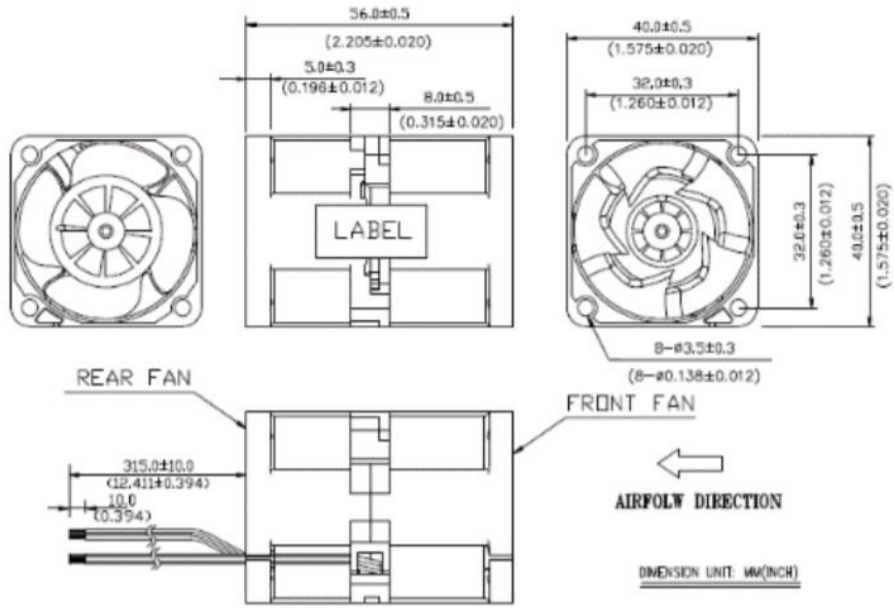


Figure 2.3: Dimensional model of Fan [4]

### 2.1.1 Ducting System

The server is provided with a removable duct which is placed in-between the fans and the PCB, in the absence of the duct, when the fans throw air it may not reach the components requiring maximum cooling and thus ducts are provided to direct the airflow towards the components requiring maximum cooling. The detailed structure of the duct is shown in the below figure 2.4.

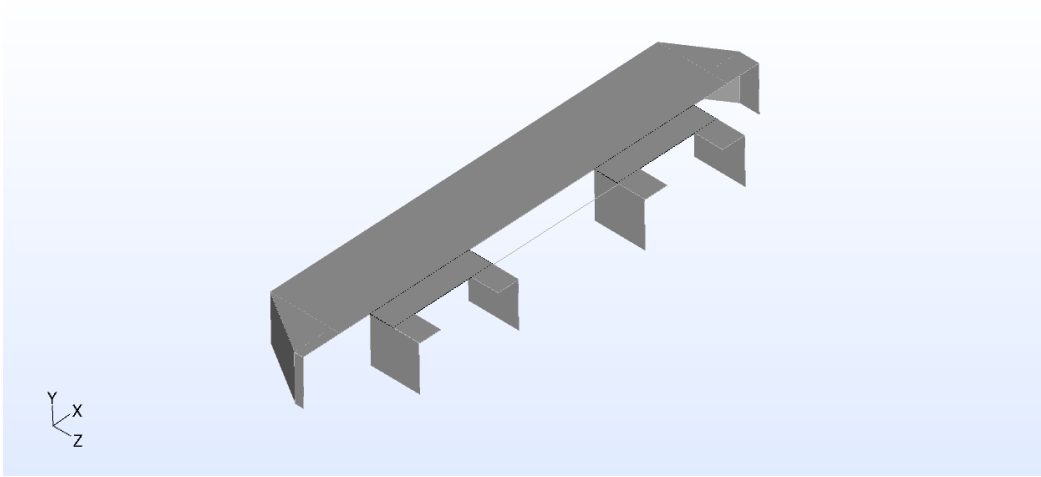


Figure 2.4: Isometric View of Duct

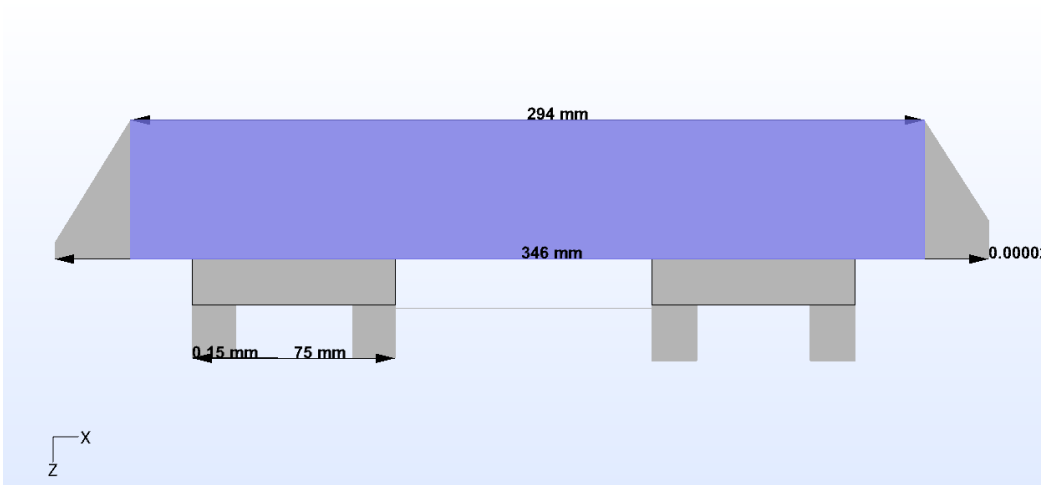


Figure 2.5: Top View of Duct

## CHAPTER 3

### Computational Fluid Dynamics (CFD) Analysis

#### 3.1 Detailed Model of the Baseline Model

This chapter showcases the CFD model and mesh sensitivity analysis to calibrate it. It is essential to calibrate the CFD model to get accurate results and thus improving the duct of the server. A detailed CFD model of the server is shown. The CFD model contains all the heat generating and flow impeding components including heatsinks, CPUs, DIMMs and chipsets.

The detailed model is shown in Figure 3.1.

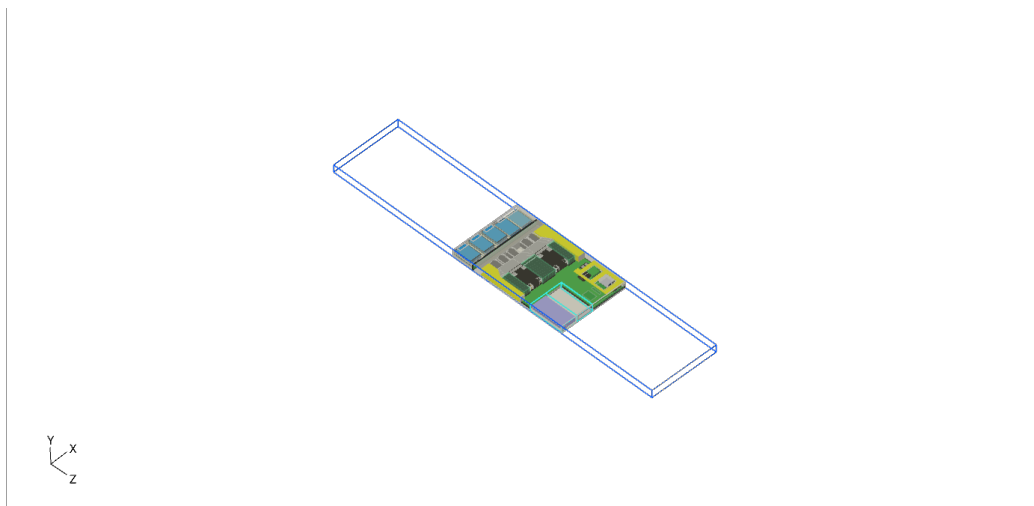


Figure 3.1: Isometric View of CFD Model

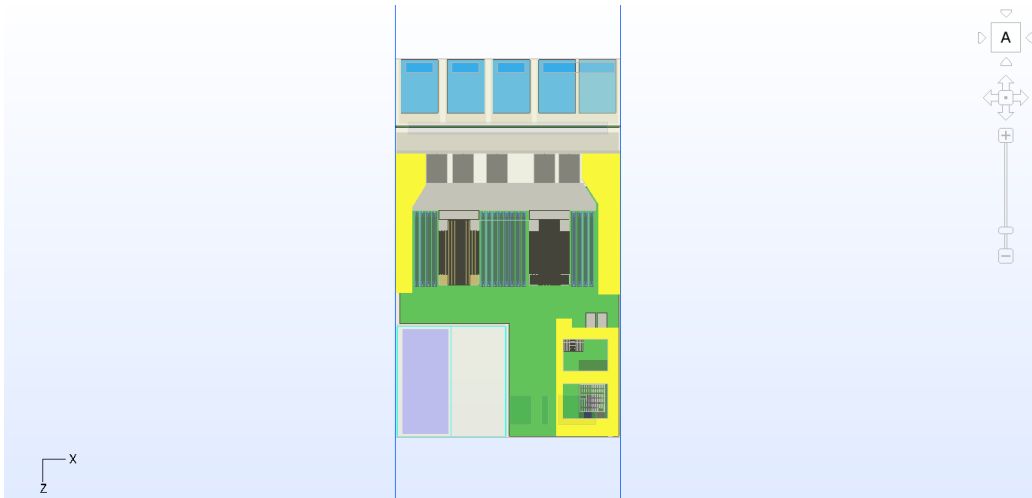


Figure 3.2: Top View of CFD Model

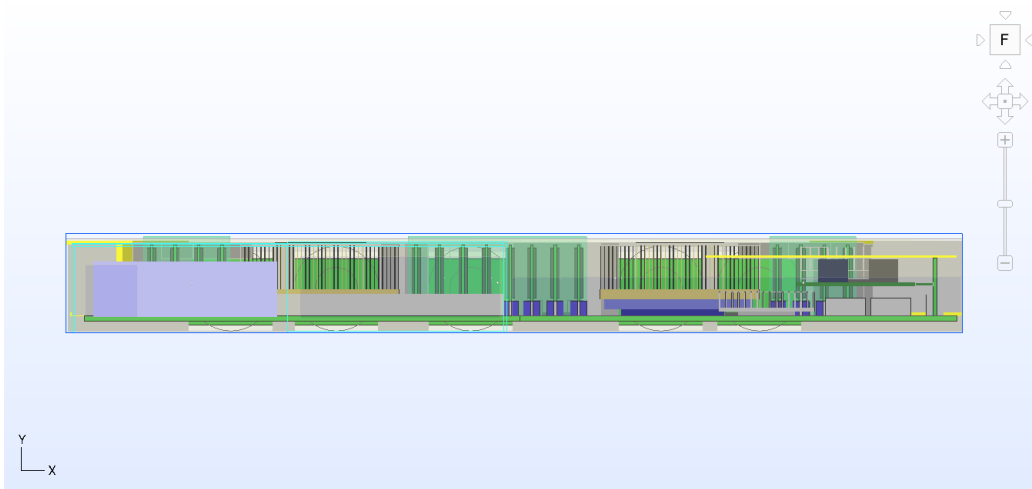


Figure 3.3: Rear View of CFD Model

Table 3.1: Thermal Design Power of the components

Device	Thermal Design Power (TDP)
CPU	135 W
DIMMs	3.5 W
Chipset	8 W
Fans	0.6-7 W
Hard Drive	5 W
Ethernet Port	6.8 W
PCIe Riser Card	6.8 W

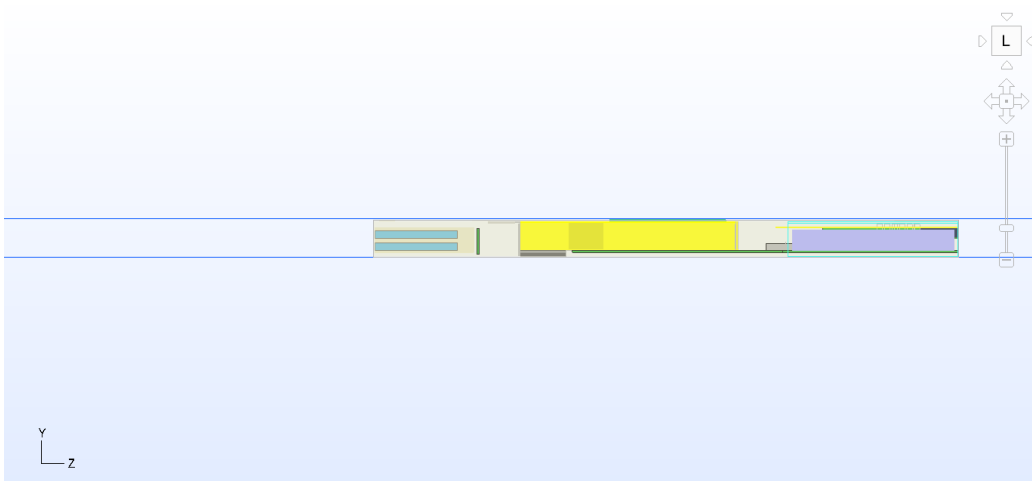


Figure 3.4: Side View of CFD Model

The thermal design power (TDP) of the heat generating components inside the server are as shown in the table 3.1.

### 3.1.1 Heatsinks

The heatsink is provided above the CPU with dimensions considered from the actual server. The model of the heatsink is shown.

Table 3.2: Heatsink Specifications

Heat Sink Specification	
Base Width	75mm
Base Depth	123mm
Base Thickness	4.6mm
Fin Height	20.6
Number of Fins	40
Material	Pure Copper (386 W/mK)

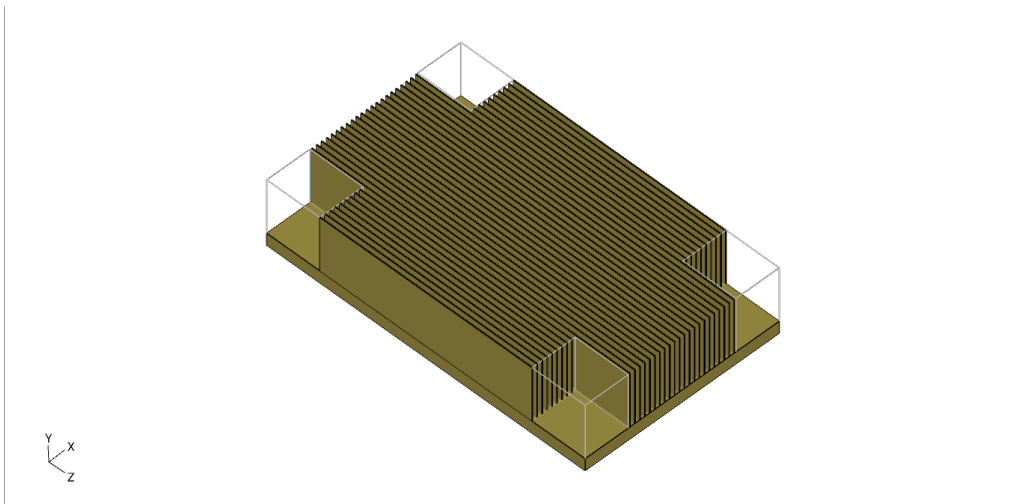


Figure 3.5: Heatsink Model for the server

The specifications for the heatsink is given in the table 3.2

### 3.2 Mesh Sensitivity Analysis

Mesh Sensitivity analysis is performed to ensure that the model is independent of the grid count. Since the system resistance is done with turning the fans off, sensitivity analysis is also done keeping the fans turned off. The analysis is done at different grid counts keeping the inlet flow rate constant. The grid count considered

are 17, 27, 46 and at 57 million grid counts with the inlet flow rate at 35 CFM and 25C temperature and keeping the rear end open to the environment.

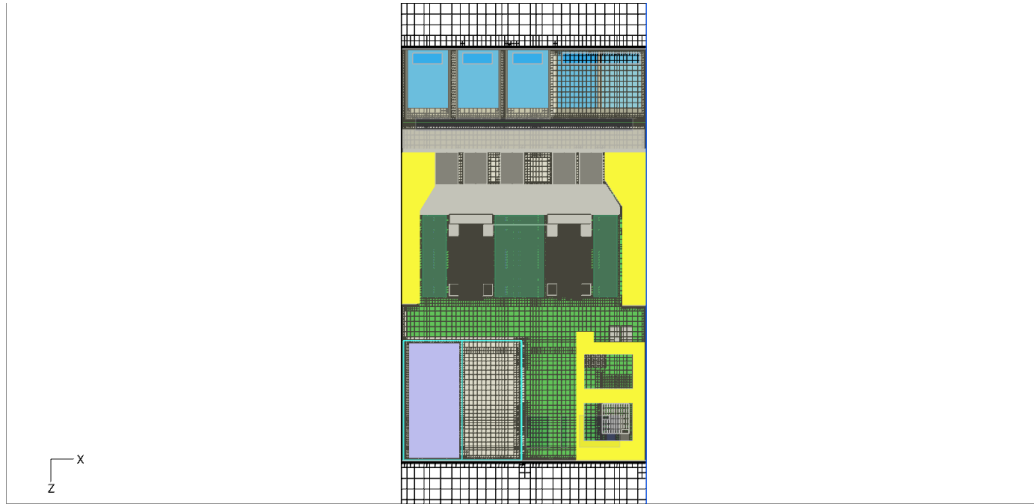


Figure 3.6: Model with 17M Grid Count

### 3.3 Flow Analysis using CFD

#### 3.3.1 System Resistance curve

The resistance occurred by the components inside the server to the flow of air creates a difference in pressure. The pressure difference at the front end and rear end is measured at varying flow rates are plotted to form the system resistance curve, to measure the inlet and outlet pressure's , three sensors are placed at the front and the rear end as shown in the figure 3.7.



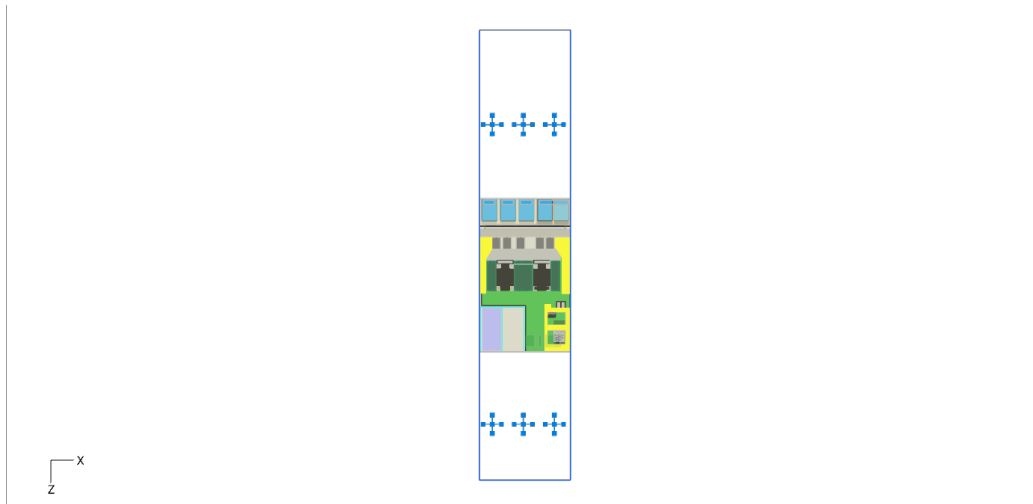


Figure 3.7: Position of Inlet & Outlet Sensor

Jay et.al showed the experimental system resistance curve and will be using it to compare the system resistance curve with the new design [5].

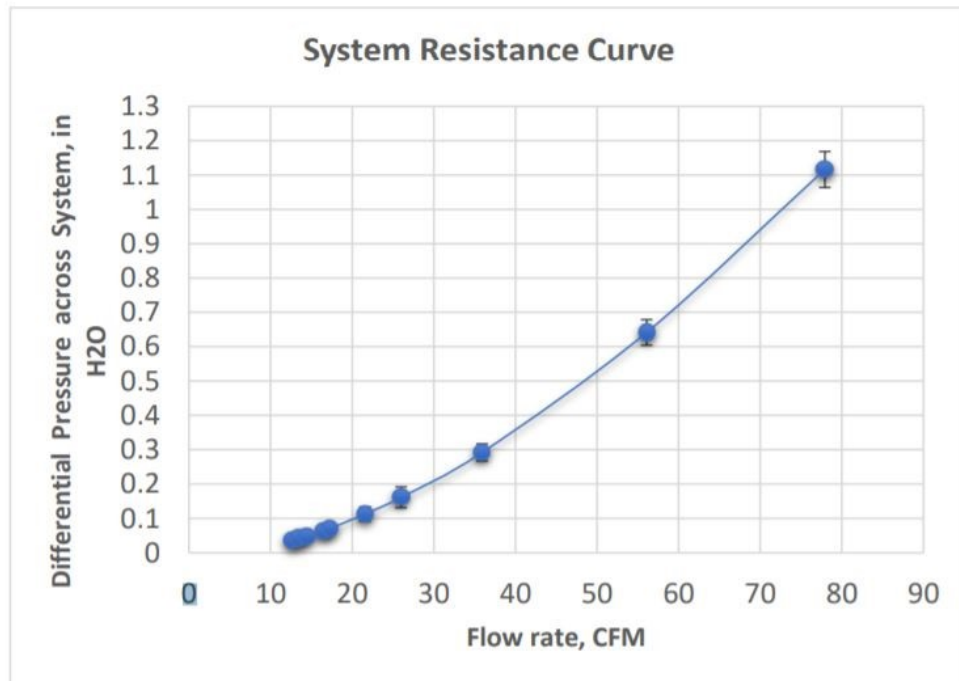


Figure 3.8: System Resistance curve for the baseline [5]

## CHAPTER 4

### Design Improvements

#### 4.1 Improvement in duct design

The calibrated model is simulated at different flow rates to understand the flow of air through the duct. It is important to supply efficient air flow to the components such as the DIMMs and CPUs. At different flow rates the simulation on the model with the original duct showed internal air recirculation which caused an increase in the temperatures readings of the components causing an increase in the fan speed and thus increasing the power consumption by them. It is important to reduce air recirculation and keeping the duct temperature into permissible limits. Therefor an optimal balance is required to improve the design of the duct. A set of fan speeds and temperature readings of the processors, DIMMs and chipsets are taken into consideration for designing new duct for the server. A set of designs are generated, and the air flow formed is studied. The simulations with the original duct showed formation of vortex on the upper region inside the duct at different flow rates. Thus, vanes on the upper region are introduced to form a streamline flow of the air and avoiding the formation of vortex on the above regions and directing the air more towards the Heatsinks and DIMMs, thin plate walls are provided to obstruct excessive places where the air gets stored and thereby reducing the flow of the air, these walls also helps increasing the velocity of air and directing air towards the components.

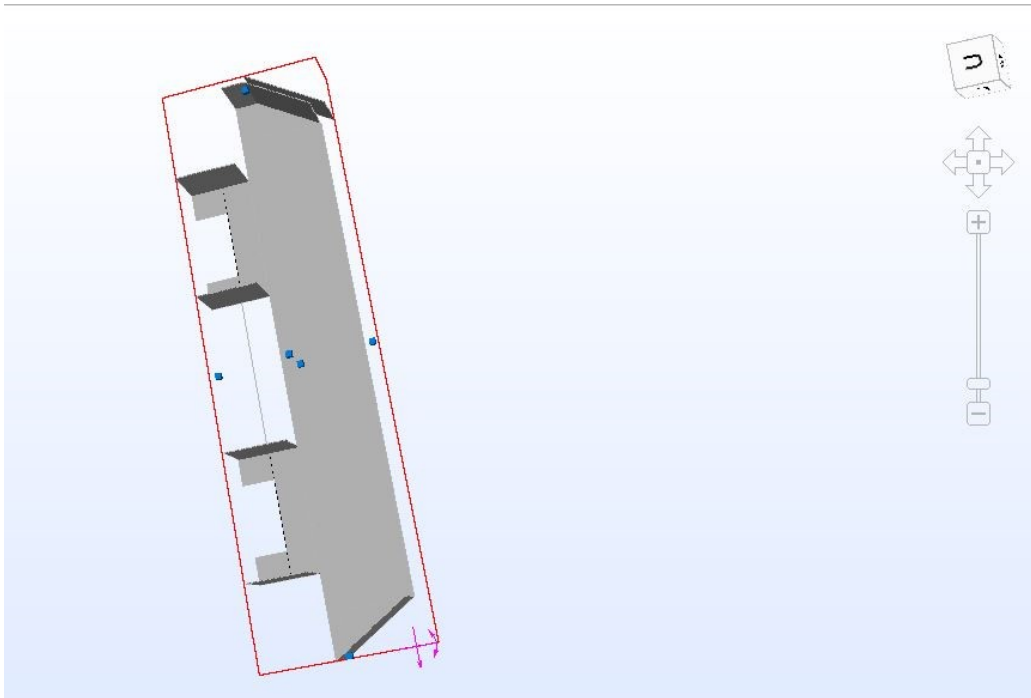


Figure 4.1: Original Duct

A set of designs with different dimensions of vanes at different locations are solved and the best design considered is the one having maximum air flow at permissible duct temperature.

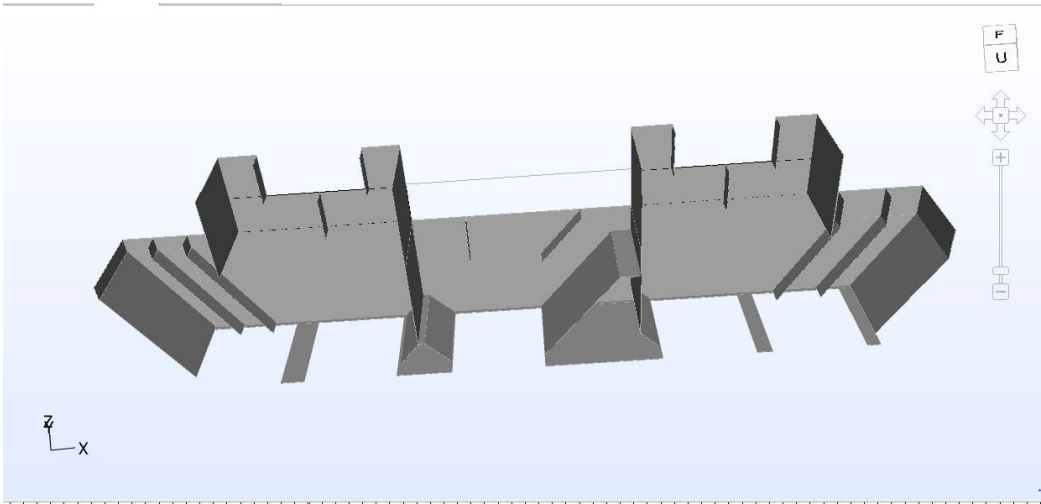


Figure 4.2: Improved Duct

The dimension of the vanes is shown in the figure 4.3.

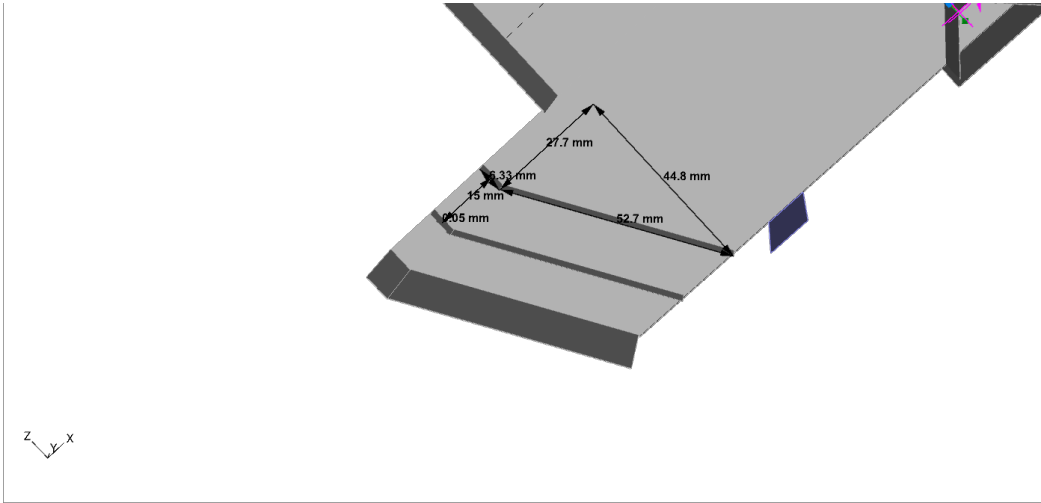


Figure 4.3: Closer View of Vanes inside Duct

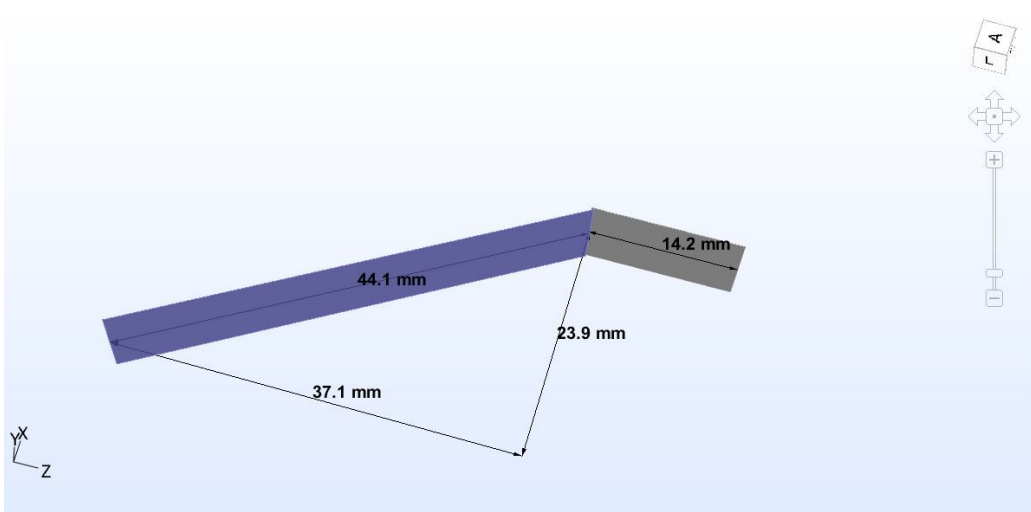


Figure 4.4: Vane dimensions

## 4.2 Improvement in Chassis design

The simulations showed that the air entering from the front end of the server passing through the drives present at the front causes an increase in the temperature before reaching the fans. It is observed that the air at 25C inlet temperature passing through the drives increased the temperature by approximately 5C, i.e the temperature before reaching the fans is getting preheated which overall decreases the cooling efficiency. It is important to provide an alternate route to the air flow or to relocate the drives inside the server which is difficult. D. Zhou et. al showed that providing an extra inlet airflow on the sides can help in lowering the component temperature. Thus, vents with holes is provided on the sides of the server [21]. The vents are placed right in-between the fans and the hot swappable back pan as shown in Figure 4.5

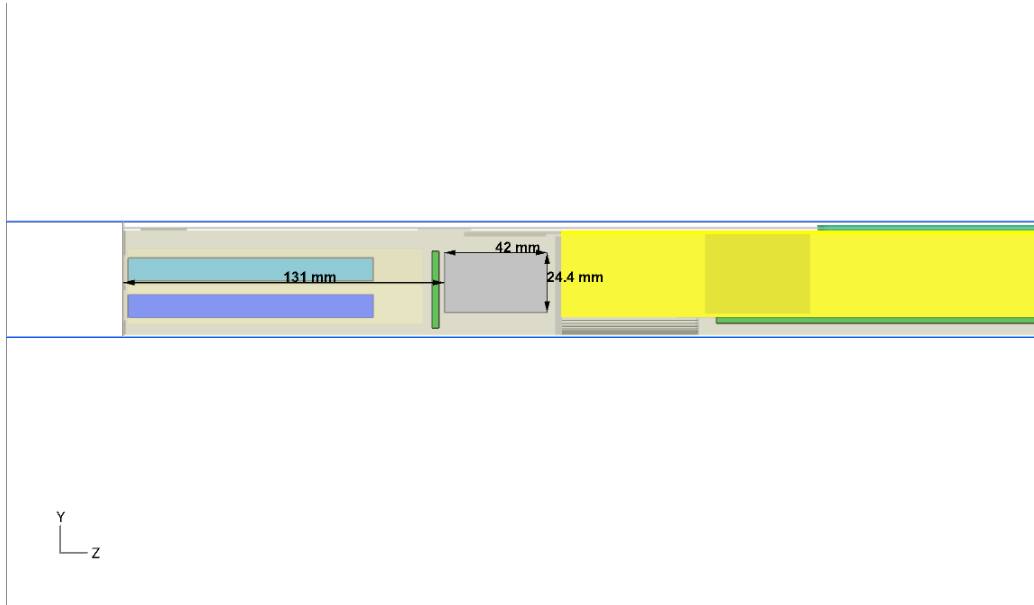


Figure 4.5: Side Vent openings

These vents on the sides help the air to bypass the drives and directly enter the area before the fans. Parametric optimization is performed at different inlet temperatures and fan speeds to determine the hole diameters and free area ratio. The higher the FAR higher will be the air flow but with the increase in the FAR could result in increased Electromagnetic Interference (EMI) emission which could result into early failure of the components and thus decreasing the lifetime of the components and an early retirement of the server. The air temperature entering from the side vents is cooler than the air entering the front end of the server since they are not preheated by the drives resulting in lower temperature of air and increasing the cooling efficiency. The different diameters considered for the side holes are 3,4,5 and 6mm and considering the Free Area Ratio (FAR) ranging from 67 % to 97% The FAR of 97 % is equivalent in consideration for honeycomb structure [22].

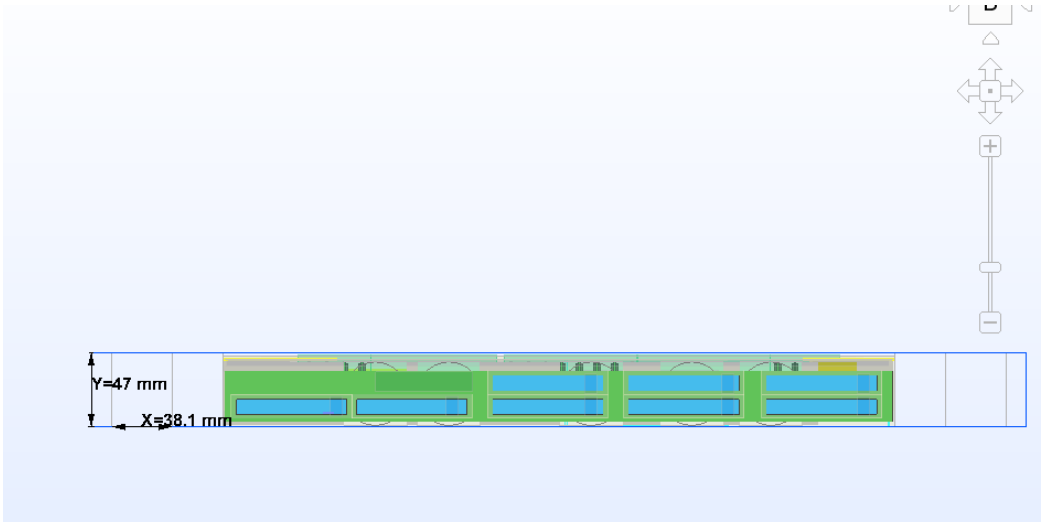


Figure 4.6: Front View of the Vent



## CHAPTER 5

### Results

#### 5.1 Mesh Sensitivity Analysis

It is necessary to do mesh sensitivity analysis to make sure that the model is grid independent to achieve accurate results. The simulations are done at different grid counts keeping the inlet temperature fix of 25C and flow rate fixed at 35 CFM and the model becomes grid independent at 27 million grid count.

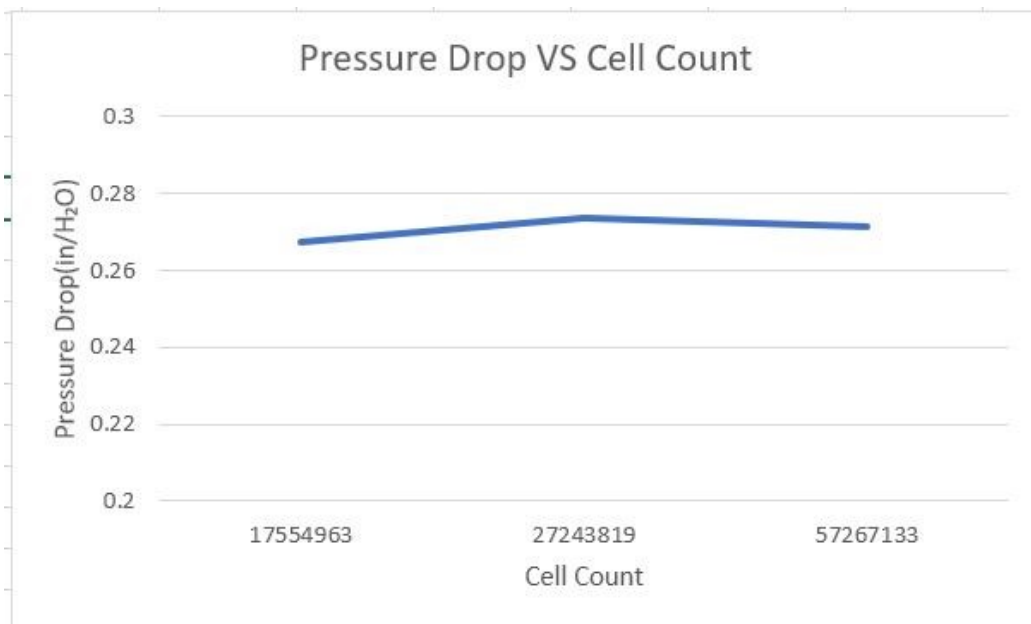


Figure 5.1: Grid independence of study of static pressure

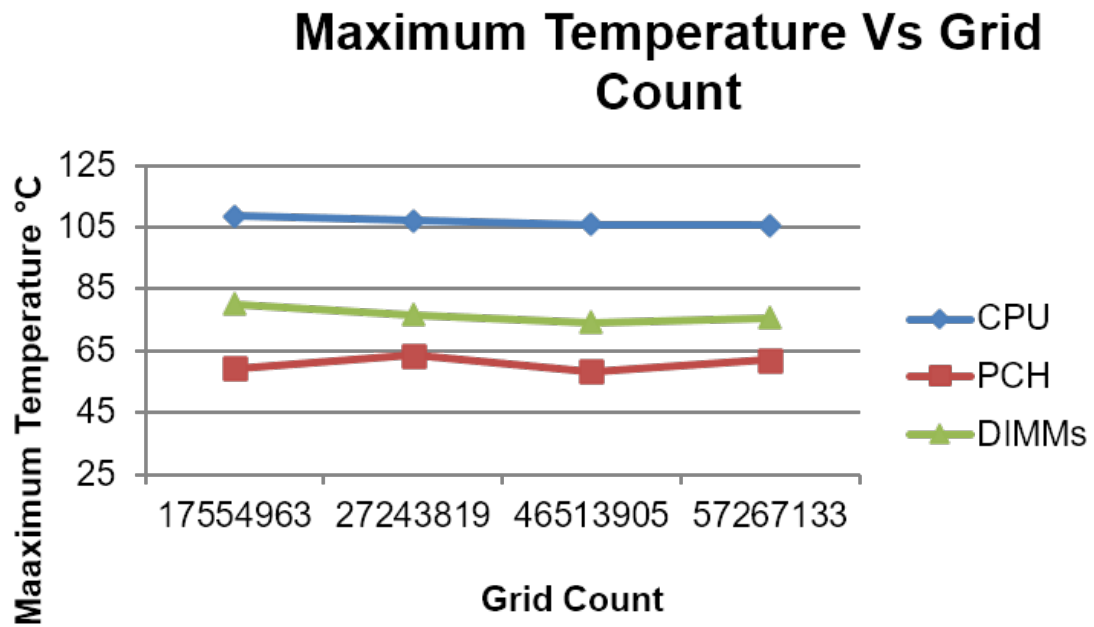


Figure 5.2: Grid independence of study of Component Temperature

## 5.2 System Resistance Curve

The system resistance curve of the new designed is compared with the baseline model to see whether the decrease in resistance

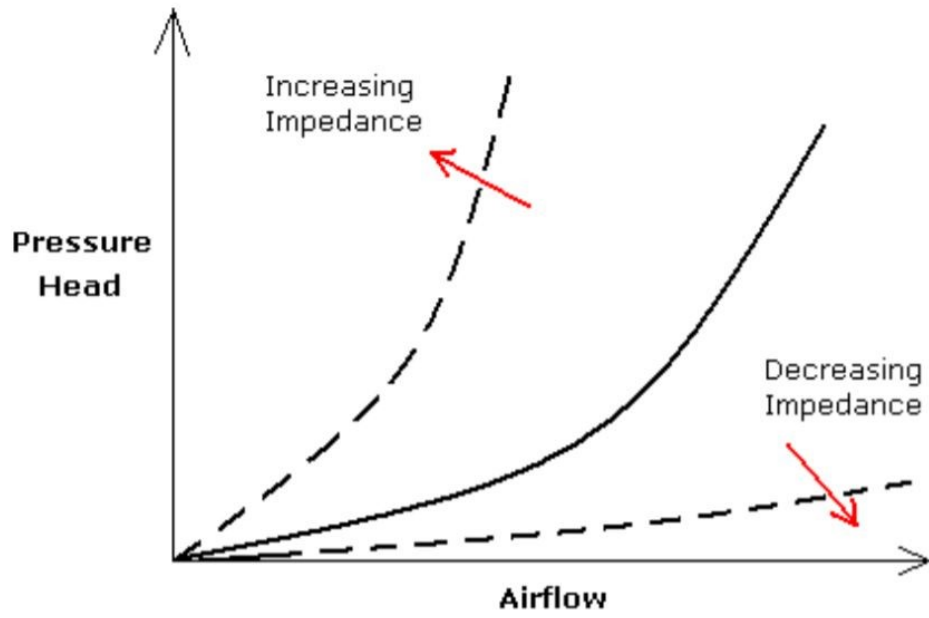


Figure 5.3: General representation of system resistance curve [6]

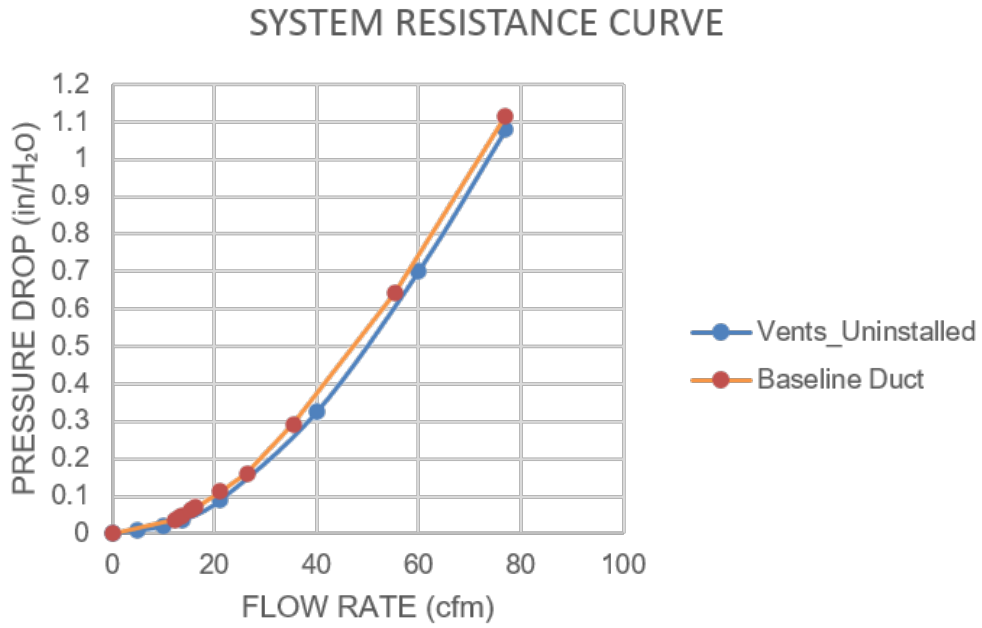


Figure 5.4: Comparison of impedance curve of Baseline Vs Improved Duct

The graph shows that there is a decrease in impedance with installing the new duct and without introducing the vents on the side walls. Now, we compare the resistance curve of the baseline model with the model with new duct and vents installed

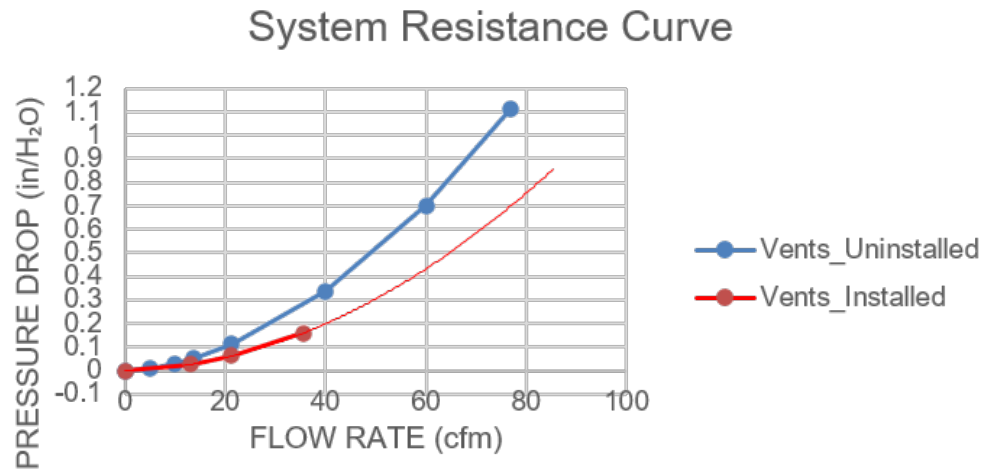


Figure 5.5: Comparison of Resistance curve of baseline model with new model

It can be seen that the improved design helps in reducing the system resistance as the pressure drop is decreasing with increasing flow rate.

### 5.3 Temperature comparison of baseline and improved design

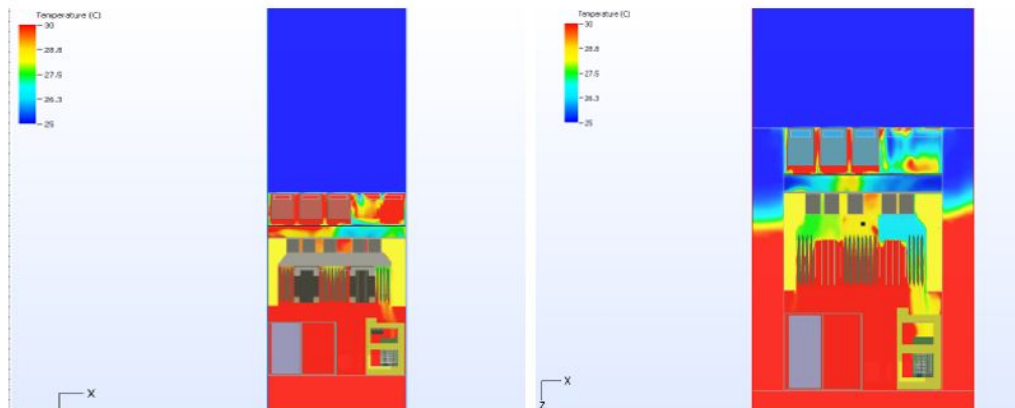


Figure 5.6: Temperature plot of the baseline and improved design model

The Temperature is set as user defined from 25C to 30C. As shown, in the temperature of the baseline model, the temperature in-between the fans and drives is higher this is because the air entering from the front side comes in contact with the hot drives and carries the heat generated by drives inside the server. It can be seen that, providing side vents helps in cooling as the air entering the server from the sides is cooler than the air entering from the front side as they do not carry the heat generated from the drives.

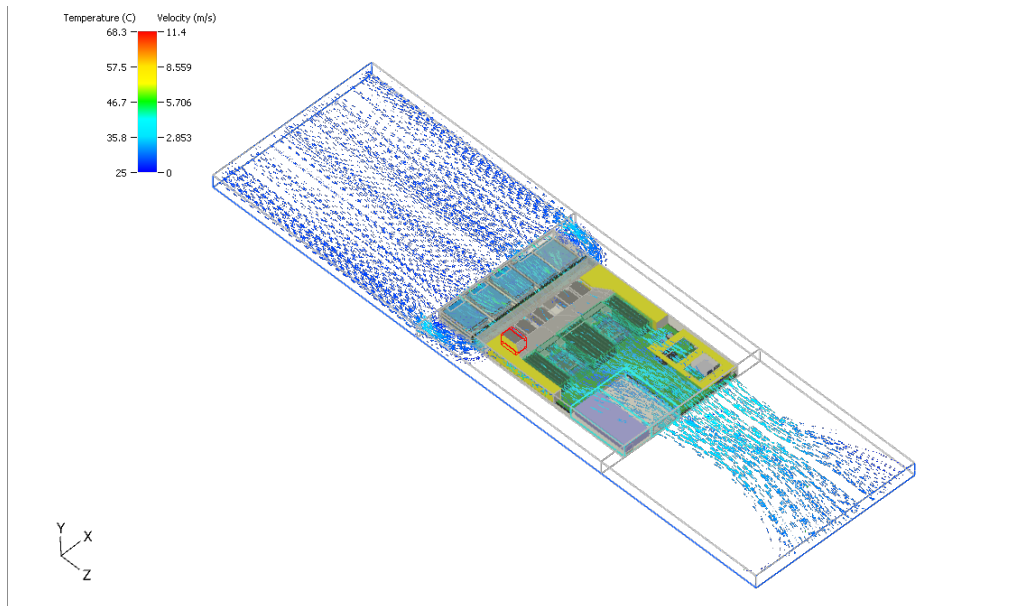


Figure 5.7

#### 5.4 Temperature comparison for different fan speeds and FAR

As shown earlier, the improved ducting and the vents provide a better cooling of the components. Thus, to validate the design we run different simulations with different Free Area Ratio and different vent hole diameters at different fan speeds. To measure the temperature components, we have placed the sensors at both CPU and at chipsets

Table 5.1: Position of Sensors

No.	Component
1	U06
2	U01
3	B1

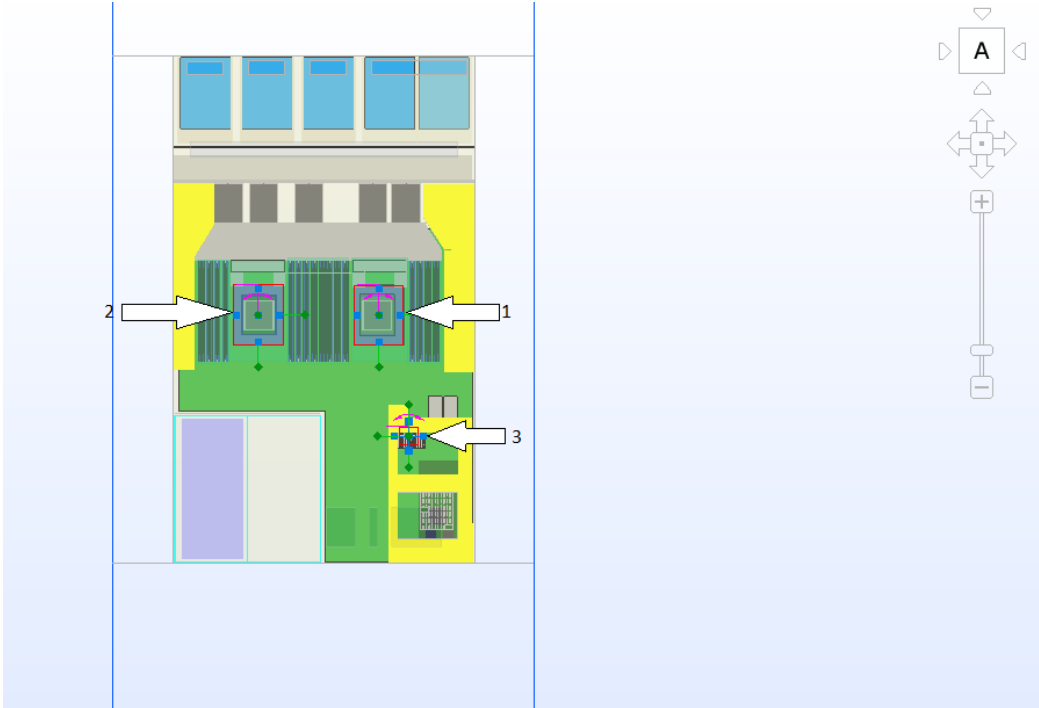


Figure 5.8: Placement of sensors

The different hole diameters selected are 3mm, 4mm, 5mm and 6mm with the free area ratio ranging from 67% to 97% at varying fan speeds from 4000 RPM to 9800 RPM

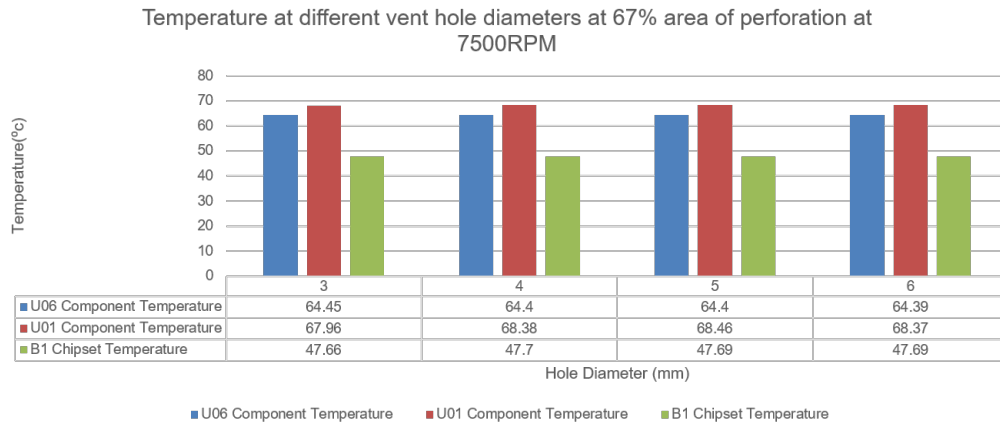


Figure 5.9: Temperature at different vent hole diameter at 67% FAR

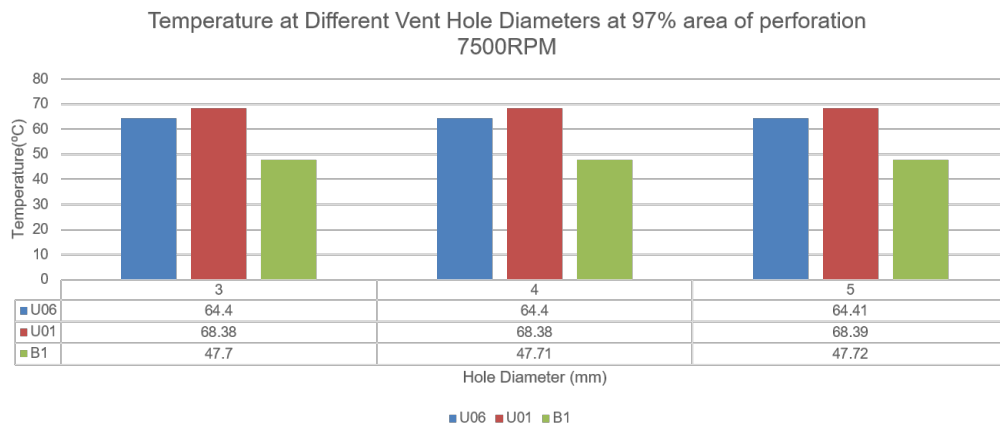


Figure 5.10: Temperature at different Vent Hole Diameters at 97 % FAR

Manasa et.al showed the temperature of processors, DIMMs and chipsets of the baseline model and we will be using it to compare the temperatures of the model with improved ducting and vent openings [23].



Table 5.2: Temperature of U06 Component at different inlet temperature

Air Inlet Temperature (C)	U06 Component Temperature (C)		Savings (%)
	Baseline	Improved design	
15	78.54	76.54	-2.5465
25	67.3	64.4	-4.3091
35	70.3	74.43	5.875
45	88.8	77.3	-12.95

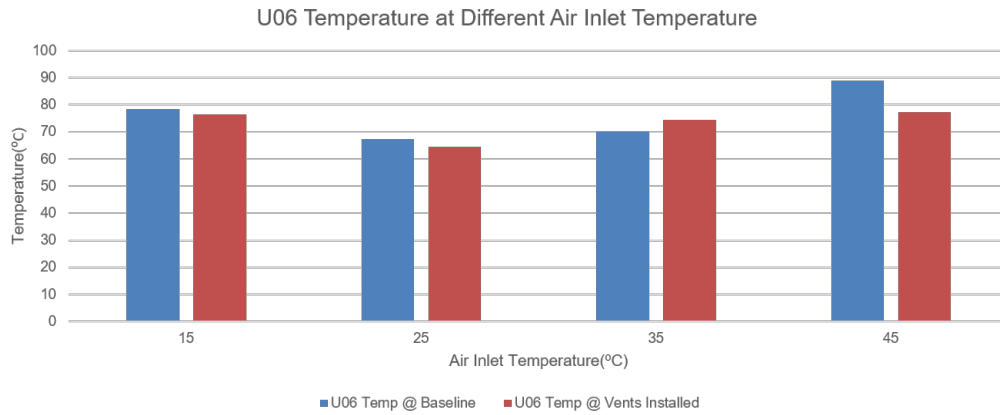


Figure 5.11: Temperature of U06 component at different inlet temperature

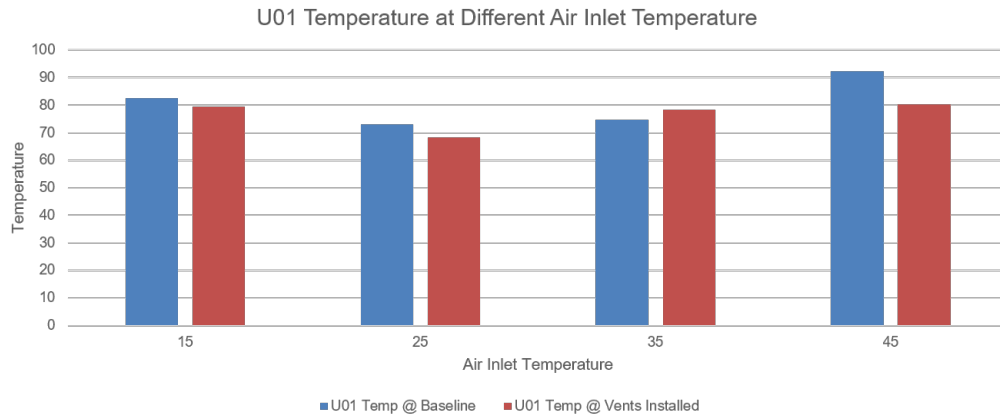


Figure 5.12: Temperature of U01 component at different inlet temperature

Table 5.3: Temperature of U01 at different inlet temperature

Air Inlet Temperature (C)	U01 Component Temperature (C)		Savings (%)
	Baseline	Improved design	
15	82.52	79.53	-3.6234
25	73.1	68.38	-6.4569
35	74.8	78.45	4.88
45	92.3	80.18	-13.131

Table 5.4: Temperature of Chipset at different inlet temperature

Air Inlet Temperature (C)	Chipset Component Temperature (C)		Savings (%)
	Baseline	Improved design	
15	59.2	51.56	-12.905
25	50.8	47.7	-6.1024
35	57	57.46	0.807
45	77	64.14	-16.701

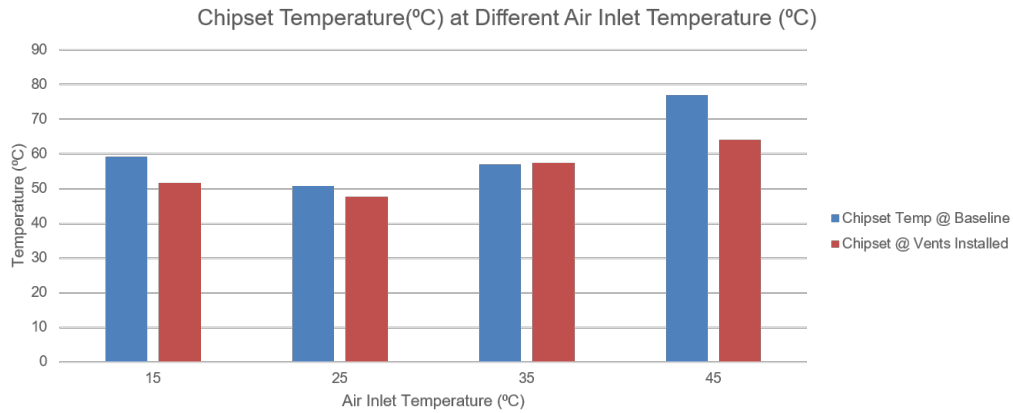


Figure 5.13: Temperature of Chipset at different inlet temperature

As seen in the above graphs the temperature of the components and chipset for new design are lower compared to the baseline model, except the temperature for components at 35C inlet temperature is higher but are under permissible limits according to ASHRAE TC 9.9 .due to the difference in fan speeds as for the baseline model the fan speed is 9500 RPM, whereas the fan speed for new model considered

is 7500 RPM helping in reducing the power consumption by the fans which will be discussed in further sections.

### 5.5 Savings achieved in Fan speeds

In this chapter, we will be comparing the fan speeds of the baseline model with the improved design model. Manasa et.al showed the fan speeds for air cooled server at 100% CPU utilization and will be using it to compare the fan speeds of baseline and with the improved model at different air inlet temperatures [23].

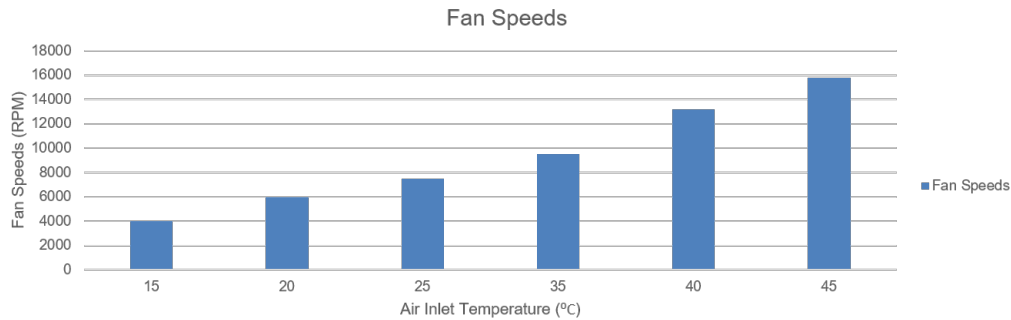


Figure 5.14

Due to the improved design, the server requires lesser air flow to maintain the component temperature within permissible limits compared to the baseline model. Figure 5.15 represents the reduction in fan speeds observed in the model with new duct.

Table 5.5: Fan speeds for the baseline and improved design

Air Inlet Temperature (C)	Fan Speeds in RPM		Savings (%)
	Baseline	Improved design	
15	4000	4000	0
20	6000	4000	-33.33
25	7500	6000	-20
35	9500	7500	-21.05
40	13200	9800	-25.75
45	15800	9800	-37.97

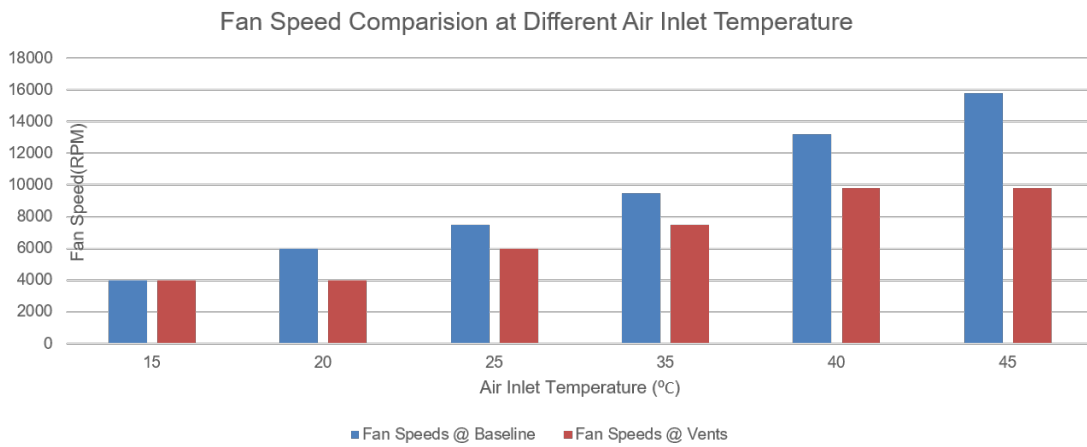


Figure 5.15: Fan speeds for the baseline and improved design

Table 5.5 represents the percentage reduction achieved in fan speed

## 5.6 Savings achieved in fan power consumption

Figure 5.16 indicates the fan power consumption in both the scenarios. As with increase in air inlet temperature the fan speeds for the improved design is lower than the baseline model. This is due to the increase in airflow from the sides which helps in reducing the fan speeds and thus reducing the power consumption.

Table 5.6: Savings in fan power consumption

Air Inlet Temperature (C)	Fan Power Consumption in Watts		Savings (%)
	Baseline	Improved design	
15	1.3723	1.3723	0
20	2.0709	1.3723	-33.734
25	2.8076	2.0709	-26.239
35	4.44	2.8076	-36.766
40	10.44	4.5901	-56.034
45	16.5	4.5901	-72.181

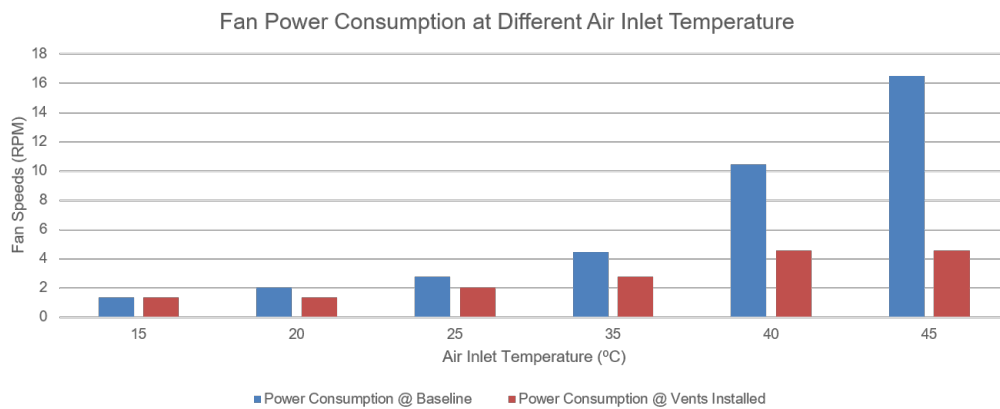


Figure 5.16: Fan Power Consumption at Different Air Inlet Temperature

## CHAPTER 6

### CONCLUSION AND FUTURE WORK

#### 6.1 Conclusion and Discussion

In this study, mesh sensitivity analysis is performed to calibrate the CFD model. The resulting calibrated model is used to parametrically improve the ducting system inside the server and redesigning the chassis by installing vents on the sides to provide more airflow to the server. Computationally improved duct and vents have helped in saving fan power consumption, fan speeds and cooling the components.

The savings achieved are listed below:

1. 26-72% of savings in achieved in fan power consumption as a result of improved ducting and vents
2. 20-38% of reduction in fan speed is achieved
3. 2.5-13% drop in temperature of U06 component has been achieved.
4. 3-13.13% drop in temperature of U01 component has been achieved.
5. 6-16% drop in temperature of Chipsets has been achieved
6. The 3mm 4mm at 97% FAR for the vent openings can be used for this server without excess EMI emissions

#### 6.2 Future Work

A valid prototype of the improved duct can be manufactured and experiments can be performed to validate the study. A rack level study can be performed with the improved ducting and redesigned chassis

## REFERENCES

- [1] Facebook engineering, “introducing data center fabric, the next-generation facebook data center network”. [Online]. Available: <https://engineering.fb.com/production-engineering/introducing-data-center-fabric-the-next-generation-facebook-data-center-network/>
- [2] “Thermal guidelines for data processing environments,” *ASHRAE Technical Committee 9.9*, pp. 1–45, 2011.
- [3] “Cisco ucs c220 m3 high-density small form factor rack server spec sheet.”
- [4] “Specification for approval,” *G. P. Battery*, pp. 1–14, 2012.
- [5] J. U. Parekh *et al.*, “Comparative rack level cfd analysis of air to hybrid cooling data center,” Ph.D. dissertation, 2019.
- [6] “Fan configuration and airflow impedance lab manual part 1 me146.” *San Jose State University*.
- [7] What is a data center - cisco, website. [Online]. Available: <https://www.cisco.com/c/en/us/solutions/data-center-virtualization/what-is-a-data-center.html>
- [8] E. Masanet, A. Shehabi, N. Lei, S. Smith, and J. Koomey, “Recalibrating global data center energy-use estimates.”
- [9] A. S. M. R. R. Chowdhury, M. Sarker, N. D. Love, and A. R. Choudhuri, *Effect of Particle Density on the Hydrodynamic Behavior of a Gas-Solid Fluidized Bed*. [Online]. Available: <https://arc.aiaa.org/doi/abs/10.2514/6.2013-4092>
- [10] R. Sarker, A. S. M. R. R. Chowdhury, N. Love, and A. Choudhuri, *Flow Field Visualization and Drag Analysis of Particles in a Gas-Solid Fluidized Bed*. [Online]. Available: <https://arc.aiaa.org/doi/abs/10.2514/6.2013-597>

- [11] M. R. H. Sarker, A. R. Chowdhury, and N. Love, "Prediction of gas–solid bed hydrodynamics using an improved drag correlation for nonspherical particles," *Proceedings of the Institution of Mechanical Engineers, Part C: Journal of Mechanical Engineering Science*, vol. 231, no. 10, pp. 1826–1838, 2017. [Online]. Available: <https://doi.org/10.1177/0954406215622652>
- [12] A. S. M. R. R. Chowdhury, "Gas-solid bed hydrodynamics of non-spherical particles," p. 114, 2014. [Online]. Available: <https://login.ezproxy.uta.edu/login?url=https://search.proquest.com/docview/1615810823?accountid=7117>
- [13] S. Ramdas, A. S. M. R. R. Chowdhury, A. Lakshminarayana, R. Bhandari, T. Chauhan, A. Misrak, and D. Agonafer, "Impact of thermal aging on thermo-mechanical properties of oil-immersed printed circuit boards," in *Proceedings of SMTA International*. Rosemont, IL, USA: SMTA, 2019, pp. 772–778.
- [14] J. M. Shah, R. Eiland, P. Rajmane, A. Siddarth, D. Agonafer, and V. Mulay, "Reliability Considerations for Oil Immersion-Cooled Data Centers," *Journal of Electronic Packaging*, vol. 141, no. 2, 04 2019, 021007. [Online]. Available: <https://doi.org/10.1115/1.4042979>
- [15] T. Chauhan, A. Misrak, R. Bhandari, P. Rajmane, A. S. M. R. Chowdhury, K. B. Sivaraaju, M. Abdulhasansari, and D. Agonafer, "Impact of thermal aging and cycling on reliability of thermal interface materials," in *Proceedings of SMTA International*. Rosemont, IL, USA: SMTA, 2019, pp. 118–123.
- [16] A. Misrak, T. Chauhan, P. Rajmane, R. Bhandari, and D. Agonafer, "Impact of Aging on Mechanical Properties of Thermally Conductive Gap Fillers," *Journal of Electronic Packaging*, vol. 142, no. 1, 11 2019, 011011. [Online]. Available: <https://doi.org/10.1115/1.4045157>
- [17] M. Chaudhari, A. S. M. R. R. Chowdhury, U. Rahangdale, A. Misrak, P. Rajmane, A. Doiphode, and D. Agonafer, "Reliability assessment of bga solder joints



- Megtron 6 vs FR4 printed circuit boards,” in *Proceedings of SMTA International*. Rosemont, IL, USA: SMTA, 2019, pp. 136–141.
- [18] U. Rahangdale, B. Conjeevaram, A. Doiphode, P. Rajmane, A. Misrak, A. R. Sakib, D. Agonafer, L. T. Nguyen, A. Lohia, and S. Kummerl, “Solder ball reliability assessment of wl CSP — power cycling versus thermal cycling,” in *2017 16th IEEE Intersociety Conference on Thermal and Thermomechanical Phenomena in Electronic Systems (ITherm)*, 2017, pp. 1361–1368.
- [19] J. Denria, P. Rajmane, and D. Agonafer, “Board level solder joint reliability assessment study of Megtron 6 vs FR-4 under power cycling and thermal cycling,” in *2018 17th IEEE Intersociety Conference on Thermal and Thermomechanical Phenomena in Electronic Systems (ITherm)*, 2018, pp. 1289–1295.
- [20] “Energy logic 2.0 new strategies for cutting data center energy costs and boosting capacity,” *Energy Network Power*, p. 2, 2007.
- [21] D. Zhou, M. Zhang, and C. Du Intel, “Enhancing rack servers air cooling capability with extra system inlet airflow through air ducts between racks,” in *2017 16th IEEE Intersociety Conference on Thermal and Thermomechanical Phenomena in Electronic Systems (ITherm)*. IEEE, 2017, pp. 857–863.
- [22] E. Chikando, E. Bodette, S. Connor, and B. Archambeault, “Vent hole size analysis for high-frequency systems chassis design,” in *2010 IEEE International Symposium on Electromagnetic Compatibility*. IEEE, 2010, pp. 813–818.
- [23] M. Sahini, U. Chowdhury, A. Siddarth, T. Pradip, D. Agonafer, R. Zeigham, J. Metcalf, and S. Branton, in *2017 16th IEEE Intersociety Conference on Thermal and Thermomechanical Phenomena in Electronic Systems (ITherm)*.

## BIOGRAPHICAL STATEMENT

Himanshu Modi was born in India. He received his Bachelor of Engineering degree in Mechanical Engineering from University of Mumbai, Maharashtra, India in June 2018. He started his Master studies in Mechanical Engineering at the University of Texas at Arlington in Fall 2018. He interned as a Mechanical Design Engineer at Gamco - A division of Bobrick from May 2019 to August 2019. He received his Master of Science in Mechanical Engineering from The University of Texas at Arlington, in May 2020. His interests include designing and thermal analysis in the field of Datacenter cooling.